Electron-magnon scattering and magnetic resistivity in 3*d* ferromagnets

B. Raquet,[1,*] M. Viret,[2] E. Sondergard,[2] O. Cespedes,[3] and R. Mamy[4]
[1]*Laboratoire National des Champs Magnétiques Pulsés (LNCMP), 143 Av. de Rangueil, 31432 Toulouse, France*
[2]*CEA, Saclay, Service de l'Etat Condensé, Orme des merisiers, 91191 Gif sur Yvette, France*
[3]*Physics Department, Trinity College, Dublin 2, Ireland*
[4]*Laboratoire de Physique de la Matière Condensée de Toulouse, 135 Av. de Rangueil, 31077 Toulouse, France*
(Received 26 November 2001; revised manuscript received 3 May 2002; published 25 July 2002)

The determination of collective spin excitations and their contribution to the intrinsic resistivity via spin-flip electronic scattering are addressed for 3*d* ferromagnets using magnetotransport experiments. We present longitudinal high-field magnetoresistance (MR) measurements from 4 to 500 K and up to 40 T on Fe-, Co-, and Ni-patterned thin films. Well above the technical saturation of the magnetization—i.e., in the paraprocess regime—we report an almost linear and nonsaturating negative MR of around 0.01–0.03 $\mu\Omega\,\mathrm{cm\,T^{-1}}$ at 300 K for the three magnets. We demonstrate its magnetic origin, and we assign this high-field resistivity decrease to the electron-magnon scattering and the spin-wave damping in high fields. We propose a theoretical calculation of the magnetic resistivity originating from spin-flip intraband *s*-*s* and *d*-*d* and interband *s*-*d* transitions via electron-magnon diffusion including both the high-field effect on the magnon spectrum and the magnon mass renormalization. Convincing agreements between the high-field measurements and our model provide a unique estimate of the pure magnetic resistivity in 3*d* ferromagnets. Our analysis also gives an insight into the low-energy spin waves—i.e., the theoretical magnon saturation field and the magnon mass renormalization consistent with neutron scattering results for the three magnets.

DOI: 10.1103/PhysRevB.66.024433 PACS number(s): 72.10.Di, 72.15.Gd, 72.25.Ba

I. INTRODUCTION

Strong 3*d* ferromagnets like Fe, Co, and Ni have been intensively studied for more than half a century in the frame of the controversy between localized and itinerant-electron theories of magnetism. Their magnetic properties like the temperature dependence of the magnetization or the high-magnetic-field susceptibility have been successfully described by the band splitting model[1–3] once major improvements have been introduced. Among them, we shall cite the temperature dependence of the spin densities of states or the existence of collective spin excitations.[4–6] With the achievement of high-energy neutron sources, inelastic neutron scattering in these metallic magnets revealed new properties of the magnon relation dispersion which validates the band ferromagnetism: in the low-temperature regime, both the temperature dependence of the spin-wave stiffness with a T^2 term[7,8] and the existence of an optic branch for magnon confirm the itinerant nature of the 3*d* magnetism.[9–11] More recent topics on 3*d* transition metals deal with the interplay of spin-polarized transport and spin-dependent scattering processes in nanostructured devices for magneto electronics. Fe, Co, and Ni layers are the most encountered ferromagnetic electrodes in magnetic devices with a spin polarization of a few tens of a percent. Recently, a study of spin polarization in cobalt-based tunnel junctions has demonstrated the 3*d* character of the tunneling electrons in Co.[12] Interesting results are also obtained on the understanding of the ''ultimate'' magnetoresistance originating from the spin-dependent scattering on nanoscale magnetic inhomogeneities like magnetic domain walls in ferromagnetic thin films.[13] The magnitude of these resistive effects is spin polarization dependent at the Fermi level and relies on the spin coupling between charge carriers and the local magnetic moment via the predominant *s*-*d* interaction. The strength of this interaction and the thermal spin disorder are thought to have a severe impact on the spin coherence length which is a critical parameter for giant magnetoresistive effects. However, despite intensive studies in the 1970's on the electronic scattering processes responsible for the resistivity in metallic ferromagnets,[14–23] the magnitude of the *s*-*d* interaction and its contribution to the magnetic resistivity via spin-flip electronic transitions remains poorly known. No experiment has inferred a direct estimate of the pure spin-flip electronic scattering contribution to the resistivity in a temperature range where spin excitations, electron-phonon scattering, and inter-electronic collisions coexist.

In this paper, we report on an original manner to determine both the nature of the spin disorder and its contribution to the intrinsic resistivity of the three ferromagnets Fe, Co, and Ni up to $T_c/2$. Whereas standard galvanomagnetic studies are performed in low fields, we measure the longitudinal magnetoresistance (MR) in epitaxial Fe, Co, and Ni thin films in a 40-T pulsed magnetic field, well above the technical saturation of the magnetization, between 1.8 and 500 K. Our measurements exhibit an almost linear and nonsaturating negative MR in the single-domain magnetic state. The resistive slope is around 0.01–0.03 $\mu\Omega\,\mathrm{cm\,T^{-1}}$ at 300 K for the three ferromagnets. We assign the decrease in resistivity to the high-field effect on the intrinsic spin disorder and its coupling to charge carriers. We demonstrate that this effect results from a reduction of electron-magnon scattering processes due to a damping of the spin waves at high fields. We propose a theoretical calculation of spin-flip electronic relaxation times via electron-magnon collision. Convincing agreement between the high-field measurements and our model ensures the consistence of the theoretical approach and provides a unique estimate of the resistivity of magnetic origin

in $3d$ ferromagnets. Our analysis also gives an insight into the low-energy spin waves—i.e., the theoretical magnon saturation field and the magnon mass renormalization involved in the electronic scattering for the three magnets.

In Sec. II after a brief summary of experimental details, we present our experimental results on longitudinal MR in Fe-, Co-, and Ni-patterned thin films as a function of field and temperature and we extract the temperature and field variation of the magnetic part of the resistivity $\Delta\rho_{\mathrm{mag}}(T,B)$. In Sec. III, following the formalism developed by Goodings,[15] we derive a theoretical expression of the magnetic resistivity in strong ferromagnetic metals based on intraband $[s\text{-}s;d\text{-}d]$ and interband $[s\text{-}d]$ spin-flip electronic transitions due to electron-magnon scattering. High-field effects on the low-energy magnons as well as the magnon mass renormalization are introduced to derive an analytical expression of the field and temperature dependence of the magnetic resistivity $\rho_{\mathrm{mag}}(T,B)$, relying on standard band structure parameters for Fe, Co, and Ni. In the last section, comparison between the experimental results and the model provides an accurate determination of (i) the spin-flip $[s\text{-}d]$ relaxation time via electron-magnon interaction up to 500 K, (ii) the high-field spin-wave damping and the magnon mass renormalization, and (iii) the magnitude of the magnetic contribution to the intrinsic resistivity.

II. EXPERIMENT AND RESULTS

Magnetoresistance is measured on Fe, Co, and Ni thin films deposited on MgO and Al_2O_3 substrates by molecular beam epitaxy (for Fe and Ni) and by thermal evaporation under ultrahigh vacuum (for Co). The films thickness range from 7 to 80 nm. A residual resistance ratio around 27 for the thicker films attests to their high structural quality. The high-field magnetotransport experiments have been performed in the LNCMP facilities (Toulouse, France), using a 40-T pulsed field with a 1-sec total pulse duration. Standard ac techniques for low-level signals were used to measure the longitudinal MR ($i\|B$) on patterned thin films. We focus here on the high-field electronic scattering regime where the intrinsic anisotropic MR and any possible giant MR due to grain boundaries have no more effects on the magnetoresistive signal.

Our systematic study of longitudinal MR (Fig. 1) on Fe, Co, and Ni thin films shows a normal MR in the low-temperature regime resulting from the well-known Lorentz force on charge carriers. A crossover from a positive to a negative resistance slope is observed as the temperature is increased. It follows the temperature-induced reduction of the electronic mean free path. In the high-temperature regime, but still well below the Curie temperature T_c, a negative MR clearly dominates the high-field signal for applied fields well above the demagnetization field of the magnet and its magnitude significantly increases with temperature. For the three ferromagnets, the MR roughly reaches -1% at 30 T for temperatures around $T_c/3$ and exhibits an almost linear field dependence for higher temperatures, with no departure toward saturation in 40 T.

It is customary to define the resistivity as a function of the

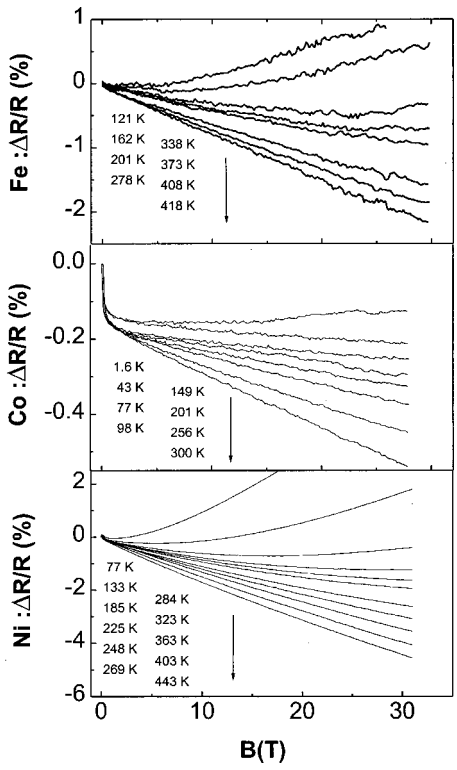

FIG. 1. Longitudinal high-field magnetoresistance ($B\|i$) at various temperatures for Fe, Co, and Ni epitaxial films $-\mathrm{Fe}_{80\,\mathrm{nm}}/\mathrm{MgO}$, $\mathrm{Co}_{7\,\mathrm{nm}}/\mathrm{Al_2O_3}$, and $\mathrm{Ni}_{20\,\mathrm{nm}}/\mathrm{MgO}$. Note the extrinsic negative MR below the technical saturation of the magnetization for Co due to grain boundary effects.

average electronic relaxation time τ and its field dependence as $\rho_{\mathrm{total}}(\tau)=c_1(1/\tau)+c_2(w_c\tau)^n$,[17] where w_c is the cyclotron frequency. The first term expresses the electronic scattering processes limiting the conductivity. The second one accounts for the positive MR with an n power law depending on τ and the applied field. In the frame of the two-current model for metallic ferromagnets,[24] even if the transition rates of the electronic diffusions originating from different scattering sources remain additive within each conduction band, some deviations to Matthiessen's rule have been pointed out.[22,23] Therefore, the term $c_1(1/\tau)$ is conveniently expressed by

$$c_1(1/\tau)=\rho_{\mathrm{imp}}+\rho_{e\text{-}e}(T)+\rho_{\mathrm{ph}}(T)+\rho_{\mathrm{mag}}(T,B)+\rho_{\mathrm{dev}}(T,B).$$

Here ρ_{imp} is the residual resistivity due to impurities, $\rho_{e\text{-}e}(T)$ is due to the electron-electron interactions (Baber term[25]), and $\rho_{\mathrm{ph}}(T)$ is the electron-phonon scattering. These three first terms are supposed weakly dependent on an applied magnetic field in the saturated magnetic state. $\rho_{\mathrm{mag}}(T,B)$ is the magnetic resistivity originating from the spin disorder, and $\rho_{\mathrm{dev}}(T,B)$ represents the deviation to Matthiessen's rule inherent to the inter band mixing. However, for pure metals, theoretical predictions estimate that, above the low-temperature regime, let us say 50 K, the deviations to Matthiessen's rule are expected to have a minor influence on the total resistivity: $\rho_{\mathrm{dev}}(T,B)$ is about one order of magnitude lower than $\rho_{\mathrm{mag}}(T,B)$ for temperatures larger than the characteristic temperature T_F for electron-magnon scattering

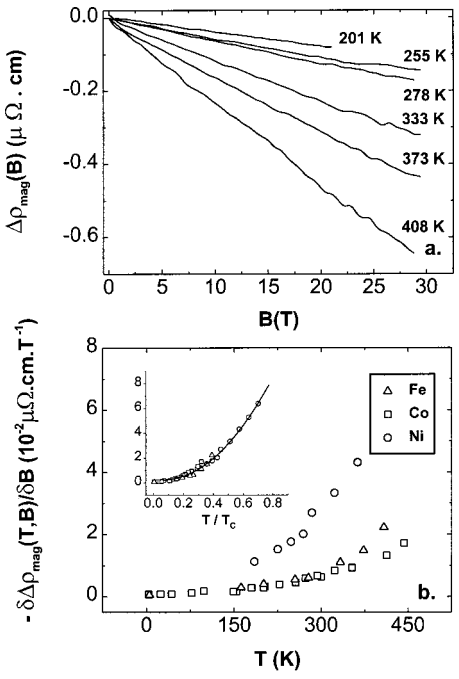

FIG. 2. (a) High-field magnetic resistivity variations deduced from the experimental MR on $Fe_{80\,nm}/MgO$. (b) High-field magnetic resistivity slopes $\partial\Delta\rho_{mag}(T,B)/\partial B|_{B\gg\mu_0 Ms}$ vs temperature for Fe, Co, and Ni. In the inset, the temperature is normalized by T_c for the three magnets.

(temperature below which the electron-magnon diffusion is frozen).[22] Therefore, in a high enough temperature range and under high magnetic fields, we make the reasonable assumption that both the normal MR and the $\rho_{dev}(T,B)$ term do not contribute significantly to the field-dependent resistivity we measure. In term of field-induced resistivity variations, we straightforwardly conclude that our results can be expressed as

$$\Delta\rho(T,B)=\rho(T,B)-\rho(T,B=0)\approx\Delta\rho_{mag}(T,B).$$

We infer a quantitative estimate of the field dependence for the pure magnetic resistivity of Fe, Co, and Ni even if its absolute value in zero field remains unknown [Fig. 2(a)]. In Fig. 2(b), we present the negative MR slopes $\partial\Delta\rho_{mag}(T,B)/\partial B|_{B\gg\mu_0 Ms}$ for the three ferromagnets in the intermediate temperature regime. For $T\approx T_c/3$, the resistivity decrease is around 0.01 $\mu\Omega\,\mathrm{cm\,T^{-1}}$. When plotted as a function of the normalized temperatures T/T_c the resistivity slopes scale on a unique curve [inset, Fig. 2(b)]. This crucial result provides strong evidence that the high-field longitudinal MR in a temperature range well below T_c is of magnetic origin. It probes the electron-spin disorder scattering processes once the Lorentz MR is negligible. It also validates the above assumptions on Matthiessen's deviations and ensures a unified picture of thermally activated spin excitations in $3d$ transition metals.

We mention that in Fig. 2(b) are plotted results obtained for Fe, Co, and Ni epitaxial thin films with various thicknesses, from 7 to 80 nm. No significant thickness dependence in this range has been observed on the magnetic resistivity variations which rules out any surface effect. To attest the intrinsic origin of the negative MR, measurements have also carried out on 1 μm Co films deposited by sputtering at room temperature and giving rise to comparable $\partial\Delta\rho_{mag}(T,B)/\partial B|_{B\gg\mu_0 Ms}$ values. Therefore, structural quality little influences the magnetic contribution to the overall resistivity. It only determines the low-temperature limit below which the normal MR overcomes the pure magnetic signal. No attempt has been made to subtract the positive MR in order to extend the temperature range in which $\Delta\rho_{mag}(T,B)$ is observable. The Khoeler law commonly used to scale the normal MR in metals does not provide reliable results versus temperature because the temperature does not simply affect the number of scatters: it also modifies their nature, like the wavelength of phonons involved in the scattering process.[26] Besides, it is worth noting that in principle the magnetic resistivity decrease is also present for low applied magnetic fields (of the order of 1 T). However, despite a tremendous number of papers on magnetotransport experiments in ferromagnets, few mention its existence[27–30] and no quantitative study has been performed. In low field, its magnitude of the order of 5×10^{-4} $\mu\Omega$ cm at 500 Oe is widely dominated by other galvanomagnetic effects related to the technical ordering of the magnetization. Therefore, an accurate estimate of the intrinsic resistivity $\rho_{mag}(T,B)$ requires magnetotransport experiments above the demagnetizing field.

Note that the negative high-field MR has to be related to the high-field magnetic susceptibility $\chi_{hf}(B)$ (Refs. 31 and 32) and the magnetization $M(B)$ in ferromagnets in the paraprocess.[33,34] Pioneer theoretical studies on $\chi_{hf}(B)$ predicted a simple way to infer the d-band density of state at the Fermi level;[31] however, it appeared that $\chi_{hf}(B)$ originates from several contributions in addition to the d-band susceptibility, including the orbital van Vleck susceptibility, the diamagnetic core contribution, and spin-wave excitations.[6,35] These various contributions associated with experimental difficulties to measure magnetization variations below 100 ppm in high fields have constituted a severe limit to the high-field $M(B)$ studies. Our approach, based on transport measurements, is an alternative way to probe the paraprocess via electron-spin disorder scattering.

III. HIGH-MAGNETIC-FIELD ELECTRON-MAGNON SCATTERING MODEL

The starting point for the longitudinal high-field MR model is to assume that the magnetic field mainly affects spin-flip electronic scattering processes. It is well known that both spin-flip and non-spin flip diffusions govern the electronic resistivity. The latter is driven by electron-phonon scattering and electron-electron interactions for which s-d interband transitions and s-d interactions play a predominant role.[20,22] The spin-flip scattering results in $s^{\pm}$-$s^{\mp}$,$d^{\pm}$-$d^{\mp}$ intraband and $s^{\pm}$-$d^{\mp}$ interband electronic transitions and necessarily involves annihilation or creation of one S electronic spin via Stoner excitations or collective spin excitations. These scattering processes are enhanced by the electronic properties of the partially filled polarized d band—i.e., its large effective mass m_d and the high electronic density of

states at the Fermi level, $n_d(E_F)$. All of them significantly contribute to the magnitude of the intrinsic resistivity in the temperature range of our study. An accurate distinction among the various contributions remain an unresolved task above 70 K: theoretical calculations rely on drastic simplifications and the resistivities exhibit very similar temperature dependences, in particular for $\rho_{e\text{-}e}(T)$ and $\rho_{\text{mag}}(T,B)$. However, we may wonder how a 40-T applied field induces a monotonous resistivity decrease well above the technical saturation of the magnetization. It certainly reduces the spin disorder and therefore increases the spin-flip electronic relaxation time. On the other hand, assuming a rigid band model, the corresponding Zeeman energy is approximately 4 meV in high field. We do not expect the field-induced band shift to be large enough to have a significant effect on the *s* and *d* densities of state at E_F. The absence of a singularity in the temperature dependence of the high-field MR also rules out *d*-band susceptibility effects on the electronic scattering. So in a first approximation we consider that high magnetic fields do not significantly alter the electron-phonon and the Baber scattering. Besides, below 500 K, both thermal and magnetic energy per spin under 40 T are much lower than the required energy for Stoner excitations—i.e., the band-splitting energy. Single-particle excitations and, *a fortiori*, their high-field dependence can be neglected for Fe and Co. Nevertheless, we argue that a 4-meV magnetic energy introduces a significant gap in the dispersion relation of long-wavelength magnons which is responsible for the reduction of magnetization up to approximately $T_c/2$.[36] These arguments are consistent with the idea that the magnetic resistivity is essentially dominated by spin-flip electronic scattering via electron-magnon collisions and our magnetotransport measurements are a direct probe of the field-induced spin-wave damping.

As an extension of Gooding's works[15] on spin disorder resistivity in zero field and low temperatures, we propose a new analytical expression for the contribution of electron-spin-wave scattering to the magnetic resistivity $\rho_{\text{mag}}(T,B)$, including high-magnetic-field effects on the spin-flip diffusion and the magnon mass renormalization for the high-temperature regime.

Gooding's model is based on two spherical energy *s* and *d* bands for which *s*-*d* transitions require spin waves whose *q* wave vectors exceed the radial distance between the two Fermi spheres k_{Fs} and k_{Fd}. The matrix elements of the interaction Hamiltonian H_{sd} between a conduction-electron $k\alpha$ and a spin-wave system is expressed by

$$\begin{aligned}&|\langle k'\alpha'^{\pm},n(q)\pm 1|H_{sd}|k\alpha^{\mp},n(q)\rangle|^2\\&\quad=\frac{2S}{N}\left(n(q)+\frac{1}{2}\pm\frac{1}{2}\right)|G_{\alpha\alpha'}(k-k')|^2\delta_{k',k\mp q}\Bigg).\end{aligned}\tag{1}$$

A $k^{\mp}$ conduction electron in an α band is scattered into a $k'^{\pm}$ electron state in an α' band with creation (or destruction) of a spin wave q ($k^{-}\rightarrow k'^{+}$) (or $k^{+}\rightarrow k'^{-}$). Here α and α' hold for the *s* and *d* conduction bands. We assume a coherent diffusion with momentum conservation, and the spin-wave umklapp processes are neglected. $n(q)$ is the number of spin waves q per unit of volume, and $G_{\alpha\alpha'}(k\text{-}k')$ is the exchange potential in the reciprocal space between the two bands α and α'. In the following calculation, we consider that the electronic interaction as a δ function. Thus $G_{\alpha\alpha'}(q)$ are constant in *k* space and contain three parameters G_{ss}, G_{dd}, and G_{sd} corresponding to the intraband and interband interaction strengths. The transition probability for $k^{\mp}\alpha\rightarrow k'^{\pm}\alpha'$ process via magnon scattering is[15]

$$\begin{aligned}&W(k\alpha^{\mp},n(q)\rightarrow k'\alpha'^{\pm},n(q)\pm 1)\\&\quad=\frac{4\pi S}{N\hbar^2}\left(n(q)+\frac{1}{2}\pm\frac{1}{2}\right)|G_{\alpha\alpha'}|^2\\&\qquad\times\delta_{k',k\mp q}\delta(E(k\alpha^{\mp})-E(k'\alpha'^{\pm})\mp E(q)).\end{aligned}\tag{2}$$

The last δ function imposes energy conservation where $E(k\alpha)$ is the energy of a conduction electron $k\alpha$ and $E(q)$, the q spin-wave energy. In the approximation of long-wavelength magnons, which will be justified later, the magnon energy has a quadratic q dependence in the central Brillouin zone and an energy gap due to the magnetic anisotropy B_A, the spin-wave demagnetization $\mu_B M_s \sin^2\theta_k$, and the internal magnetic induction B_{int} (Ref. 17):

$$E(q)=Dq^2+g\mu_B(B_{\text{int}}+B_A+\mu_B M_s\sin^2\theta_k).\tag{3}$$

Here D is the exchange stiffness, B_{int} the external magnetic induction B plus $\mu_0 M_s$, and θ_k the direction of propagation of the magnon with respect to the magnetization M_s. As we focus on the high-field study, well above the technical saturation of the magnetization ($B\gg\mu_0 M_s$), both the anisotropy energy and the spin-wave demagnetization are negligible compared to the 4-meV energy due to $g\mu_B B$ in high field. To account for the temperature dependence of spin waves, we introduce the magnon mass renormalization in the stiffness and the high-magnetic-field dispersion relation we will use is

$$E(q,T,B)\approx(D_0-D_1T^2-D_2T^{5/2})q^2+g\mu_B B.\tag{4}$$

The increase of the effective magnon mass with temperature has two contributions: a T^2 term due to the temperature dependence of the Fermi distribution and a $T^{5/2}$ variation expressing a higher corrective term due to magnon-magnon interactions.[7] Here D_0 is the zero-temperature magnon mass; D_1/D_0 and D_2/D_0 are constants of the order of 10^{-6} K^{-2} and 10^{-8} $\text{K}^{-5/2}$ for Fe.[8]

The calculation of $\rho_{\text{mag}}(T,B)$ is based on the standard derivation of the Boltzmann equation and the application of the variational method which yields a $\rho_{\text{mag}}(T,B)$ value by excess. Since steps of the calculation closely follow earlier works,[15] only the major differences in the analytical treatment due to magnon mass renormalization and the high-field effects are detailed. Using Colquitt's notation,[37] the stationary solution of the conductivity σ is equal to

$$\sigma\approx 2D_s+2D_d-(L_{ss}+M_{ss})-(L_{dd}+M_{dd})+2M_{sd}.\tag{5}$$

The terms D_s and D_d represent the rate of change of the distribution functions of the *s* and *d* conduction electrons due

to the electrical potential ε: $D_\alpha \approx \frac{2}{3} e\varepsilon V v_\alpha n_\alpha \Phi_\alpha$, where n_α is the density of state at the Fermi energy, v_α the Fermi velocity of electrons in the α band, V is the sample volume, and Φ_α is the variational function. L_{ss} and L_{dd} correspond to the intraband $s^{\mp} \rightarrow s^{\pm}$ and $d^{\mp} \rightarrow d^{\pm}$ spin-flip electron-magnon scattering via the G_{ss} and G_{dd} exchanges, whereas M_{ss} and M_{dd} are connected to the interband $s^{\mp} \rightarrow d^{\pm}$ and $d^{\mp} \rightarrow s^{\pm}$ scattering effects within the D_s and D_d conductivities, respectively. The M_{sd} term is less intuitive: it represents a coupling between the two s and d electronic channels. It is worth mentioning that Gooding's approach is not antinomic to the two-spin-current model. The s and d bands act like two spin-polarized conductivity channels with intraband and interband spin-flip transitions. The coupling term M_{sd} has a strong analogy with the spin-mixing resistivity calculated by Fert for electron-magnon interactions.[18] With little algebra on Eq. (5), the general expression of $\rho_{\mathrm{mag}}(T,B)$ for a cubic ferromagnet with one low-energy acoustic magnon branch becomes

$$\rho_{\mathrm{mag}}(T,B) \approx \frac{V\varepsilon^2}{kT} \frac{(L_{ss}+M_{ss})(L_{dd}+M_{dd})-M_{sd}^2}{(L_{ss}+M_{dd})D_d^2+2M_{sd}D_sD_d+(L_{dd}+M_{dd})D_s^2}. \tag{6}$$

As we include the magnon mass renormalization and the high-field effects on the magnon spectrum, L_{ss}, M_{ss}, L_{dd}, M_{dd}, and M_{sd} are temperature and field dependent. We derive substantially different expressions compared to former works;[15,37] they are presented in the Appendix.

Solving the integrals, Eqs. (A5) and (A6), and after successive simplifications of Eq. (6), we infer an analytical and compact form of the magnetic resistivity $\rho_{\mathrm{mag}}(T,B)$:

$$\rho_{\mathrm{mag}}(T,B) \approx \rho_0 \theta^2(T) \mathcal{R}^*_{sd}(T,B) \frac{\mathcal{T}^*_{sd}(T,B)(1+k_{Kd}/k_{Ks})+m_d/m_s\mathcal{T}^*_{dd}(T,B)}{m_d/m_s\mathcal{T}^*_{dd}(T,B)\,\theta(T)+\mathcal{R}^*_{sd}(T,B)\tilde{k}^2a^2}, \tag{7}$$

where

$$\rho_0 = \frac{3\pi VSm_dG_{sd}^2}{4N\hbar E_F e^2 (k_F a)^2}, \quad \theta(T,B) = \frac{a^2kT}{D(T)},$$

$$\tilde{k}^2 = k_{Kd}^2 + k_{Kd}^3/k_{Ks} + k_{Kd}^5/k_{Ks}^3 + k_{Kd}^6/k_{Ks}^4,$$

$$\mathcal{R}^*_{sd}(T,B) = -\ln\{\tanh[x_{\min sd}(T,B)]\},$$

$$\mathcal{T}^*_{sd}(T,B) = 2\,\mathrm{diln}\{\exp[-x_{\min sd}(T,B)]\} - \frac{1}{2}\mathrm{diln}\{\exp[-2x_{\min sd}(T,B)]\} - \frac{\mu_B B}{kT}\mathcal{R}^*_{sd}(T,B),$$

$$\mathcal{T}^*_{dd}(T,B) = 2\,\mathrm{diln}\{\exp[-x_{\min dd}(T,B)]\} - \frac{1}{2}\mathrm{diln}\{\exp[-2x_{\min dd}(T,B)]\} - \frac{\mu_B B}{kT}\ln\{\tanh[x_{\min dd}(T,B)]\}.$$

$x_{\min dd}$ and $x_{\min sd}$ are the field-induced gaps normalized by kT in the magnon dispersion relation for $d^{\mp}$-$d^{\pm}$ and $s^{\mp}$-$d^{\pm}$ transitions:

$$x^{\min dd}_{\min sd}(T,B) = \frac{D(T)q^2_{\min dd \atop \min sd} + g\mu_B B}{2kT}.$$

The final expression, Eq. (7), we obtain provides a quantitative estimate of the magnetic resistivity $\rho_{\mathrm{mag}}(T,B)$ in $3d$ ferromagnets due to electron-magnon scattering, including the magnon mass renormalization and the high-field magnetoresistance. It relies on the standard band structure parameters which allow a direct comparison with the experimental high-field resistivity we measure. One can notice that our Eq. (7) at zero field and neglecting both the magnon renormalization and the exchange splitting between the d^+ and d^- bands leads to a similar result as that obtained by Gooding.[15]

Our $\rho_{\mathrm{mag}}(T,B)$ expression brings the following general comments.

(i) The $s^{\mp}$-$s^{\pm}$ intraband scattering: The contributions to the magnetic resistivity originating from $s^{\mp}$-$s^{\pm}$, $d^{\mp}$-$d^{\pm}$, and $s^{\mp}$-$d^{\pm}$ transitions are obviously not additive. However, in the calculation, terms expressing the $s^{\pm}$-$s^{\mp}$ intraband scattering are negligible relative to the $d^{\pm}$-$d^{\mp}$ and $s^{\pm}$-$d^{\mp}$ transitions. The inefficiency of this interaction in terms of scattering stems from the large m_d/m_s ratio in $3d$ transition metals: the electron-magnon scattering affects the conductivity much more once heavy d electrons are involved in the spin-flip processes. So the s-s terms have been neglected for compactness in Eq. (7), with no alteration of the final result.

(ii) The interplay between the different parameters in $\rho_{\mathrm{mag}}(T,B=0)$: It is of interest to understand the respective effects of the band structure parameters and the expression for spin waves on the magnitude of the magnetic resistivity and its temperature dependence. In zero field, the $\rho_{\mathrm{mag}}(T)$ value, at a given temperature, is an increasing function of m_d, $n_d(E_F)$, the effective spin S, the magnon mass, and the exchange constants $G_{\alpha\alpha}$. The last term reinforces the intraband and interband electronic transitions and appears squared in $\rho_{\mathrm{mag}}(T,B)$. Unfortunately, little is known of the G_{ss}, G_{dd}, and G_{sd} values. They are thought to range between 0.2 and 0.4 eV for free atoms,[38] whereas, for $3d$ metals, the energies deduced from indirect exchange coupling theories are around 1–3 eV.[39] For convenience, we assume that the three parameters are equal around 0.5–1 eV. Here $\rho_{\mathrm{mag}}(T,B=0)$ is also strongly influenced by the spin-wave exchange stiffness D, which defines the collective spin excitations involved in the scattering process. In first order, the prefactor of Eq. (7) is roughly proportional to D^2. For a given magnon energy $E(q)$, related to a thermal activation kT, the corresponding q magnon has a larger q vector for

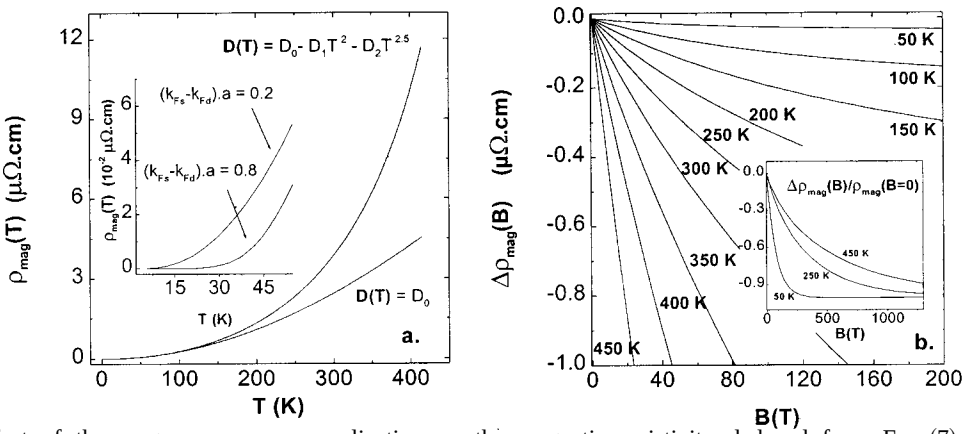

FIG. 3. (a) Effect of the magnon mass renormalization on the magnetic resistivity deduced from Eq. (7), $\rho_{\mathrm{mag}}(T)$, with $D_0 = 350$ meV Å^2, $D_1/D_0 = 2.5\times10^{-6}$, and $D_2/D_0 = 2\times10^{-8}$. The band structure parameters used for the calculation are those for iron (Table I). In inset, effect of the *k* gap between the *s* and *d* bands on the temperature dependence of $\rho_{\mathrm{mag}}(T)$ in the low-temperature regime. (b) High-field magnetic resistivity calculated for different temperatures, from 50 to 450 K. In the inset, very-high-field theoretical MR exhibiting the saturation field of the magnon damping with the iron parameters.

heavier spin waves. However, short-wavelength magnons are responsible for larger diffusion angles in the scattering process, inducing a reduction of the spin-flip relaxation time. That is why the magnetic resistivity is a decreasing factor of *D*. The temperature dependence of the magnetic resistivity is roughly driven by two terms acting in distinct temperature ranges. For temperatures lower than $Dq^2_{\mathrm{min}\,dd}$ and $Dq^2_{\mathrm{min}\,sd}$, spin waves do not have high enough energy to induce $d^{\mp}$-$d^{\pm}$ or *s*-*d* electronic transitions and $\rho_{\mathrm{mag}}(T)$ tends exponentially to zero below the energy gap. The zero field $\rho_{\mathrm{mag}}(T)$ variation is mainly defined by the intraband $d^{\mp}$-$d^{\pm}$ and the interband *s*-*d* gap values in *k* space [inset, Fig. 3(a)]. For higher temperatures, the magnon mass renormalization has a severe effect on the temperature variation of $\rho_{\mathrm{mag}}(T)$ [Fig. 3(a)]. A larger temperature dependence observed in $\rho_{\mathrm{mag}}(T)$ is a straightforward consequence of the temperature-induced enhancement of the magnon mass. The temperature effect on the spin-wave spectrum is therefore a crucial parameter for an accurate estimate of $\rho_{\mathrm{mag}}(T)$.

(iii) The low-energy magnon approximation: The upper limits of the integrations over *q* space in Eqs. (A5) and (A6) refer to the highest-energy magnon thermally excited and involved in the spin-flip process, for coherent scattering. In terms of normalized energy, the upper limit for the integrals is $2Dk_F^2/kT$, which was replaced by infinity in the calculation. If we perform the calculation of $\rho_{\mathrm{mag}}(T)$ with a finite value—i.e., restricting the accessible high-energy magnon—the result could give information on the magnon energy range which does effectively affect the electronic diffusion at a given temperature. In that respect, we estimate the magnetic resistivity as a function of an artificially high-energy cut off in the dispersion relation. From the determination of the required magnon energy to reach the total value of the magnetic resistivity, we infer that below 300 K, the low-energy magnon approximation remains justified: the main part of the resistivity comes from electron-magnon scattering with magnon energies below 150 meV. Up to such energies, the predominance of the acoustic mode with a quadratic *q* dependence has been experimentally confirmed for both Fe, Co, and Ni.[9–11] In contrast, at higher temperatures, more than 20% of the total magnetic resistivity involves magnon energies above 200 meV. Even if such magnons are statistically rare, they are supposed to have a large impact on the electronic relaxation time. The open question is to know whether the spin waves we probe by transport measurements equally affect the magnetization and the electronic spin diffusion. For Fe and Ni, high-energy neutron diffraction reveals a broadness of the acoustic branch above 150 meV due to interactions with Stoner excitations and the existence of an optical mode for *q* vectors larger than the zone center.[9–11] Therefore, considering a single quadratic acoustic mode in our model is a rather crude approximation for the high-energy magnon spectrum in the high-temperature regime; it tends to somehow underestimate the electron-magnon scattering.

(iv) The magnetoresistance: The field dependence of the magnetic resistivity is directly related to the field induced gap in the magnon dispersion relation which reduces the number of collective spin excitations. Huge magnetic fields are theoretically necessary to fully suppress electron-magnon scattering processes. Using the standard band structure parameters for iron (Table I), we estimate that the magnon saturation fields vary from 80 T at 50 K to 2000 T at 450 K [inset, Fig. 3(b)]. These large values are a straightforward consequence of the role in the scattering processes of magnons of high energy compared to the Zeeman energy induced by the applied field. The temperature dependence of the high-field MR exhibits a strong increase of $\Delta\rho_{\mathrm{mag}}(T,B)$ as the temperature increases [Fig. 3(b)]. This is only due to the enhancement of the magnetic resistivity value in zero field with temperature. We also point out that the negative MR is not quite linear; a curvature in the field dependence is always present and is band structure dependent. The shape of the $\Delta\rho_{\mathrm{mag}}(B)$ curve is mainly driven by the minimum wave vector between the Fermi spheres—i.e., the minimum magnon energy responsible for spin-flip $s^{\mp}$-$d^{\pm}$ and $d^{\mp}$-$d^{\pm}$ electronic transitions. A stronger field dependence with a larger curvature is observed for small gaps in *k* space between the $s^{\mp}$ and

$d^{\pm}$ bands. This is consistently explained by the field effects first damping the lowest-energy magnon involved in the scattering process.

(v) Other models: Since the 1950's, various models have dealt with the field dependence of the resistivity in magnetic metals and semiconductors.[21,40,41] The spin fluctuations responsible for the *s*-electron scattering are derived from the spin correlation functions including the longitudinal and transverse spin susceptibility.[21,41] In the low-field regime ($\mu_B B \ll kT$), models for $\rho(B)$ yield a linear resistivity decrease for $T \ll T_c$ (Refs. 21 and 40) and a $B^{2/3}$ dependence near T_c (Ref. 21). In our model, we only deal with transverse spin fluctuations which restricts the validity range to $T \leqslant T_c/2$. However, our calculation, based on the standard *s*-*d* interaction, takes into account the *s* and *d* conducting channels with an explicit calculation of the interband $s^{\pm}$-$d^{\mp}$ electronic transitions. It provides a more realistic description of the magnitude of the magnon induced spin-flip scattering to be compared with experimental results.

In the remainder of the paper, Eq. (7) will be used to fit the data. However, this expression being rather complicated, we propose an approximate expression for the resistivity in the paraprocess, above the low-temperature regime. For $\chi^{\min sd}_{\min dd}(T,B)<1$, which typically corresponds to experimentally accessible magnetic fields (<100 T) and above about $T_c/5$, Eq. (7) is straightforwardly transformed to a simple analytical form

$$\Delta\rho(T,B) \approx \rho(T,B) - \rho(T,0) \propto \frac{BT}{D(T)^2} \ln\left(\frac{\mu_B B}{kT}\right). \quad (8)$$

We conclude that, for a band ferromagnet, the high-field resistivity driven by the electron-magnon scattering, roughly follows a $B\ln(B)$ dependence. From the above expression, we get the temperature dependence of the MR slopes:

$$\left.\frac{\partial \Delta\rho_{\mathrm{mag}}(T,B)}{\partial B}\right|_{B \gg \mu_0 Ms} \propto T(1+2d_1T^2)(\ln T + cte),$$

where *cte* is a temperature-independent term and $d_1 = D_1/D_0$. We checked that this simplified temperature dependence constitutes an excellent approximation to the experimental MR slopes.

IV. COMPARISON WITH EXPERIMENTAL RESULTS

Our experimental MR measurements expressed in term of variation of magnetic resistivity [Figs. 2(a) and 2(b)] are compared to the theoretical expression for the magnetic resistivity deduced from the electron-magnon scattering model. As Eq. (7) relies on a significant number of parameters describing the *s*- and *d*-band structures plus the collective spin excitations, our strategy consists in fixing the band structure parameters for Fe, Co, and Ni to the most commonly admitted values of E_F, k_{Fs}, k_{Fd}, m_d/m_s, G_{sd}, and *S*. Only the magnon mass and its renormalization (D_1,D_2) are considered free parameters to account for both the magnitude of the experimental $\Delta\rho_{\mathrm{mag}}(B)$ curves, their curvature, and temperature dependence.

TABLE I. Band structure parameters for Fe, Co, and Ni used for the magnetic resistivity calculations, Eq. (6).

	V/N (10^{-23} cm^3)	E_F (eV)	$k_{Fs}\times a$	$(k_{Fs}-k_{Fd})\times a$	m_d/m_s	S	G_{sd} (eV)
Fe	1.18	7.1	3.37	0.48	9	1	0.7
Co	1.1	7.3	3.47	0.57	14	0.77	0.8
Ni	1.09	7.3	3.46	0.14	22	0.5	1.3

For iron thin films, the high-field resistivity decrease has been accurately measured from 160 to 450 K. Table I summarizes the band structure parameters we use for the fit. The major uncertainty is due to the exchange potential value G_{sd} which is a square-multiplicative term in the prefactor of $\Delta\rho_{\mathrm{mag}}(B)$. However, its value does not affect the shape of the temperature and field dependence. An excellent agreement is obtained between the high-field electron-magnon model and the experimental MR, both in terms of field and temperature dependence (Fig. 4 and inset). From the fit procedure, we infer the magnon stiffness and its temperature renormalization for iron films:

$$D(T) = (350 \pm 20)[1 - (2.5 \pm 0.2)\times 10^{-6} T^2] \text{ meV Å}^2.$$

The simplified expression [Eq. (8)] also leads to a very good fit to the data [Fig. 2(b), solid line] with a second-order term $d_1 \approx 4\times 10^{-6}$, in good agreement with the magnon mass renormalization. The extrapolated magnon mass at 0 K is fully consistent with other experimental values obtained by neutron scattering.[8,42,43] The negative coefficient we find for the T^2 dependence is also in agreement with theoretical predictions;[7] very few experimental values are available,

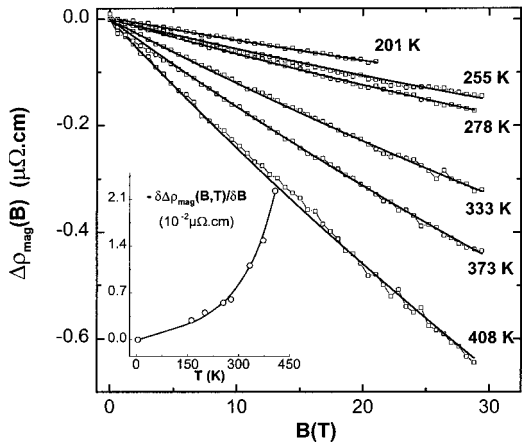

FIG. 4. Experimental high-field magnetic resistivity (open squares) and theoretical $\Delta\rho_{\mathrm{mag}}(B)$ curves (solid lines) deduced from Eq. (7) for $Fe_{80\,nm}$/MgO thin films with the band structure parameters listed in Table I and the magnon mass renormalization as only fitting parameters (see text). In the inset, the agreement between the experimental temperature dependence of the high-field MR slope (open circles) and the theoretical one (solid line).

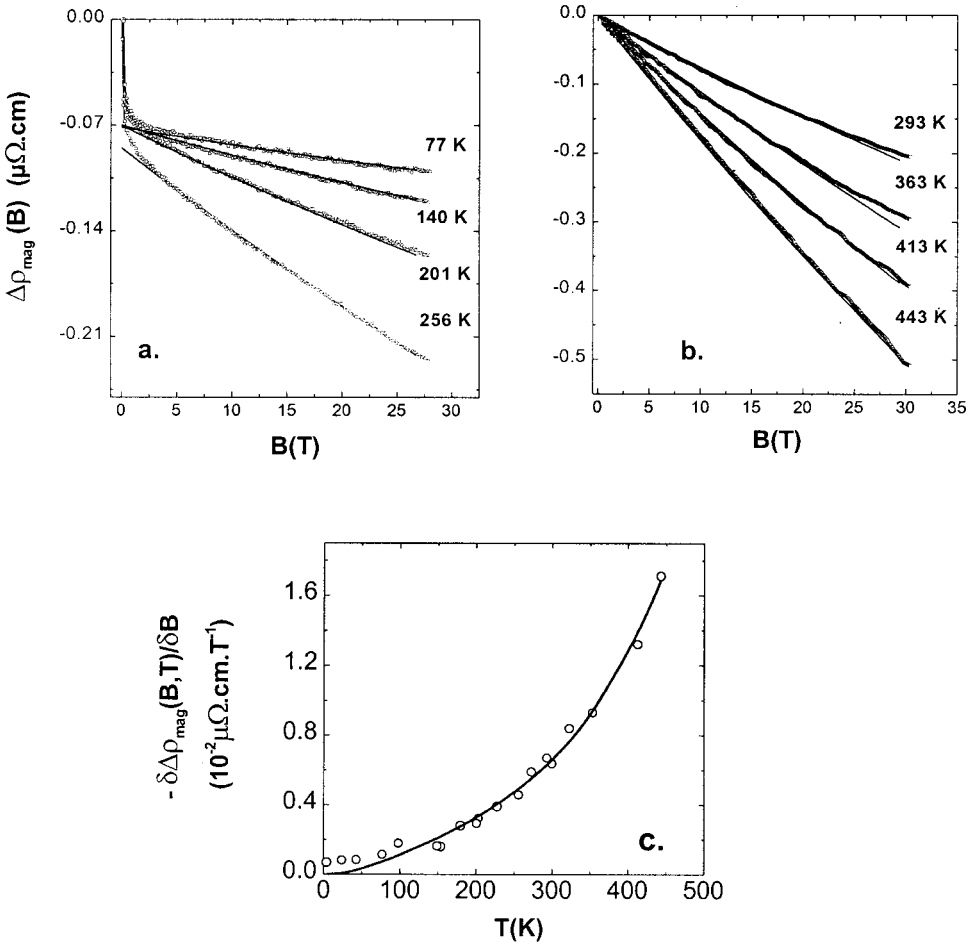

FIG. 5. Experimental high-field magnetic resistivity (open circles) and theoretical $\Delta\rho_{mag}(B)$ curves (solid lines) deduced from Eq. (7) for $Co_{7\,nm}/Al_2O_3$ (a) and $Co_{10\,nm}/Al_2O_3$ thin films (b) with band structure parameters listed in Table I and the magnon mass renormalization as unique fit parameters for both samples (see text). In (c), the agreement between the experimental temperature dependence of the high-field MR slope (open circles) and the theoretical one (solid line) for the two samples.

ranging from 1.4×10^{-6} to 5×10^{-6}.[8,44] Let us mention that the $T^{5/2}$ corrective term due to magnon-magnon interactions has little influence on the $D(T)$ variation below $T_c/3$. Its value is within the uncertainty we get in the fitting parameters. Therefore, from the temperature range and the fitting procedure, we cannot extract the $T^{5/2}$ coefficient of the magnon mass renormalization for Fe and Co.

The same analysis is performed on cobalt; we model the high-field MR obtained for different Co films [Figs. 5(a) and 5(b)] by the theoretical expression of the electron-magnon scattering in high field, relying on the standard band structure parameters for Co (Table I). Good agreements [Figs. 5(a)–5(c)] between Eq. (7) and the experimental data are obtained from which we deduce the collective spin excitations in cobalt:

$$D(T)=(470\pm20)[1-(1.5\pm0.2)\times10^{-6}T^2]\ \text{meV Å}^2.$$

We note that the experimental measurements from 4.2 to 450 K include several Co polycrystalline layers, with thickness varying from 6 to 20 nm (not all shown here). Within the full temperature range, a unique stiffness value is used for all the Co samples. The collective spin excitations are therefore little dependent on the structural properties and thickness. Even for the thinnest films, we do probe a bulk effect. The extrapolated stiffness value at 0 K is in full agreement with previous data obtained by Brillouin[45,46] and neutron scattering[47,48] and ranging from 435 to 540 meV Å^2, depending on crystallographic orientations. The average value we find is consistent with the absence of in-plane texture in the Co films we measure. The magnitude of the T^2 term, around -1.57×10^{-6} K^{-2}, also agrees with theoretical calculations.[7]

The analysis is somehow more complex for Ni films. The temperature range where we unambiguously measure the negative MR with a negligible normal MR contribution is 180–450 K. The highest of these temperatures reaches $0.7T_c$ which is too high for the simple picture of collective spin excitations we depict. Figure 6 presents the experimental high-field MR and the results of the electron-magnon model for the band structure parameters of Ni listed in Table I. We shall notice that the rather high experimental values of $\Delta\rho_{mag}(B)$ are accounted by Eq. (7) only if essential parameters like the exchange integral G_{sd} or the effective spin are little boosted. Similar conclusions have been reached by Gooding in the view of the low curves $\rho_{mag}(T)$ he obtained with the ''standard'' band structure parameters.[15] Only for G_{sd} equal to 1.3 eV (which belongs to the upper theoretical accessible values) is a satisfactory agreement obtained between our model and the high-field MR. The magnon mass and its renormalization we extract from the fits are

$$D(T)=(390\pm20)[1-(1.5\pm0.2)\times10^{-6}T^2+(6.4\pm0.2)\times10^{-8}T^{5/2}]\ \text{meV Å}^2.$$

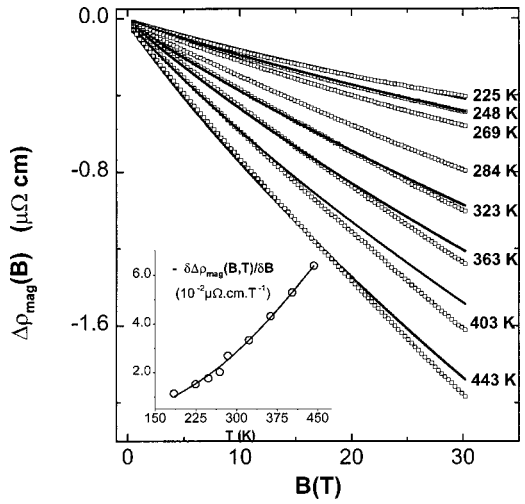

FIG. 6. Experimental high-field magnetic resistivity (open squares) and theoretical $\Delta\rho_{\mathrm{mag}}(B)$ curves (solid lines) deduced from Eq. (7) for $Ni_{20\,nm}$/MgO thin films with the band structure parameters listed in Table I and the magnon mass renormalization as the only fitting parameters (see text). Note the high-field discrepancy above 20 T for $T>T_c/2$. In the inset, the agreement between the experimental temperature dependence of the high-field MR slope (open circles) and the theoretical one (solid line).

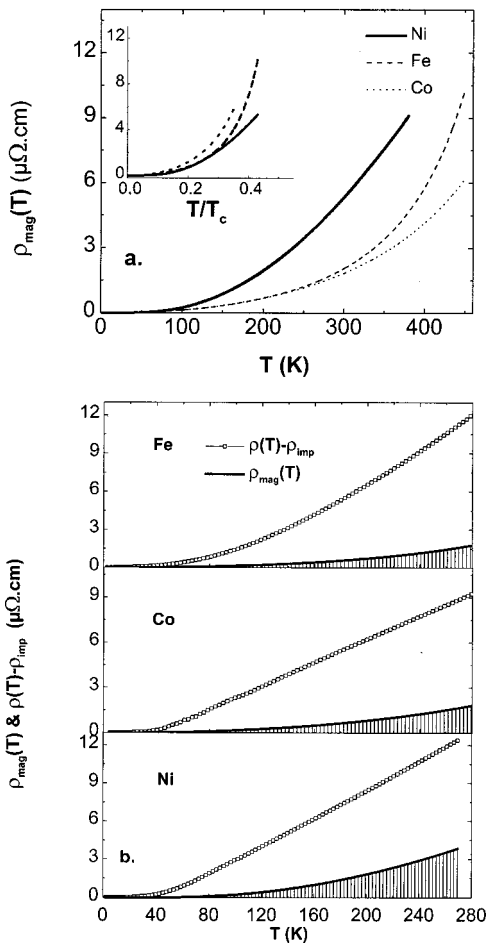

FIG. 7. (a) Determination of the magnetic resistivity due to electron-magnon scattering for Fe, Co, and Ni, from Eq. (7) relying on the adequate band structure parameters and collective spin excitations inferred from the high-field MR measurements. In inset, the magnetic resistivity as a function of the normalized temperature T/T_c. (b) Contribution of the estimated magnetic resistivity to the experimental resistivity after subtraction of the residual resistivity for Fe, Co, and Ni.

Like for Fe and Co, the spin-wave stiffness value extrapolated to 0 K agrees with neutron scattering studies.[8,49] The temperature dependence we infer is also consistent with theoretical predictions[50] and the value of the $T^{5/2}$ term we obtain is positive, as expected for a large number of *d* band electrons.[8] To the best of our knowledge, these values constitute the first experimental estimate of the Ni magnon mass renormalization. However, for $T>T_c/2$, we notice on Fig. 6 that the theoretical $\Delta\rho_{\mathrm{mag}}(B)$ curves exhibit a larger curvature in high field than the experimental ones. A significant discrepancy is observed for MR curves above 320 K and 20 T. The model for electron-magnon scattering underestimates the spin disorder in Ni films above $T_c/2$. This is not surprising, as approaching T_c, both optical magnons and Stoner excitations start to be thermally populated which enhance the spin disorder. To account for the magnetic resistivity decrease in high field above $T_c/2$, short-range spin fluctuations and a broadness of the spin-wave dispersion relation should be included in the spin-flip scattering model.

V. DISCUSSION

The convincing consistence between calculations and experimental data, based on very few parameters, strongly supports the validity of the high-field electron-magnon scattering model we developed. For Fe, Co, and Ni, the temperature dependence of the magnetic part of the resistivity can be estimated using Eq. (7) with spin-wave characteristics extracted from the high-field measurements [Fig. 7(a)]. The measurements provide evidence that the high-field slope we measure does originate from magnon damping in high field which reduces spin-flip electron-magnon scattering events. We also demonstrate that an accurate determination of collective spin excitations is accessible by magnetotransport experiments via the electron-spin disorder diffusion. At room temperature, we conclude that the electron-magnon scattering contribution to the resistivity reaches 1.8, 2, and 5.2 $\mu\Omega$ cm for Co, Fe, and Ni, respectively. The surprisingly high-temperature dependence we observe for Ni mainly comes from the small *k* gap between the $s^{\mp}$-$d^{\pm}$ bands which determines the frozen temperature T_F for electron-magnon $s^{\mp}$-$d^{\pm}$ scattering. The large magnitude and the well-pronounced curvature of $\Delta\rho_{\mathrm{mag}}(B)$ below $T_c/2$ imply small gaps in the *k* space. The frozen temperature for $s^{\mp}$-$d^{\pm}$ transitions we infer for Ni is $T_{Fsd}\approx 15$ K, which is far below the temperatures we obtain for Fe and Co, $T_{Fsd}\approx 160$ K (Fe) and $T_{Fsd}\approx 250$ K (Co). For $d^{\mp}$-$d^{\pm}$ electronic transitions, the frozen temperatures we deduce for the three magnets are around 40 K, in rough agreement with former estimates in the frame of the spin mixing calculation for the two-current model.[18] If we plot the magnetic resistivities versus the normalized temperature T/T_c, the dispersion of the $\rho_{\mathrm{mag}}(T)$ curves for Fe,

Co, and Ni is strongly reduced even if substantial differences in the temperature dependence remain [inset, Fig. 7(a)]. For instance, at $T=T_c/4$, the corresponding magnetic resistivities equal 1.2, 2.5, and 1.2 $\mu\Omega\,\mathrm{cm}$ for Fe, Co, and Ni, respectively. The success of the crude scaling by T_c makes sense as the magnitude of the band splitting which drives the spin-flip *s-d* transition roughly follows the Curie temperature. Besides, it is worth noting that above the frozen temperatures, the magnetic resistivity we infer exhibits a temperature dependence stronger than the well-known T^2 law for electron-magnon scattering as a consequence of the magnon mass renormalization.

Comparing the estimated $\rho_{\mathrm{mag}}(T)$ to the experimental resistivity $\{\rho(T)-\rho_{\mathrm{imp}}\}$ we measure, we probe the magnetic contribution to the total electronic scattering [Fig. 7(b)]. At room temperature, the spin-flip scattering via magnon is responsible for 15%, 18%, and 30% of the total resistivity for Fe, Co, and Ni, respectively (after subtraction of the residual resistivity ρ_{imp}).

The theoretical $\Delta\rho_{\mathrm{mag}}(B)$ curves in the very-high-field regime can also be extrapolated to infer an estimate of the magnetic field necessary to fully damp the spin waves, i.e., to depopulate the magnons and decrease the magnetic resistivity close to zero. For Fe and Co, the saturation fields are roughly identical, of the order of 80, 500, and 1500 T for temperatures of 20, 100, and 300 K, respectively.

VI. CONCLUSION

The general behavior of nonsaturation of magnetotransport measurements in the paraprocess regime in ferromagnets has been addressed. We demonstrate that the resistivity decrease in high field, of the order of 0.01–0.03 $\mu\Omega\,\mathrm{cm\,T^{-1}}$ at 300 K for Fe, Co, and Ni, is due to a reduction of the spin-flip electron-magnon scattering induced by damping of spin waves. A new expression has been developed for the magnetic resistivity based on intraband and interband spin flip transitions due to magnon scattering with a band structure consisting of two polarized *s* and *d* bands. The analytical expression of $\rho_{\mathrm{mag}}(T,B)$ [Eq. (7) or the simplified equation (8)] includes temperature and magnetic field effects on collective spin excitations, and it relies on the standard band structure parameters of the 3*d* ferromagnets. The model we propose is successfully applied to the experimental high-field negative MR. It ensures a unified picture for spin waves and the *s-d* interaction in the 3*d* ferromagnets. From the magnetotransport measurements, direct comparison with the high-field spin-flip model gives an estimate of the magnon stiffness and the temperature-induced renormalization for Fe, Co, and Ni in agreement with neutron experiments. The electronic transport analysis is therefore an accurate manner to probe the spin disorder above the technical saturation of the magnetization as well as the strength of the *s-d* interaction. Finally, from the parameters we extract from the high-field fits, we can estimate the contribution to the total resistivity due to the electron-magnon scattering in a large temperature range where electron-phonon and electron-electron diffusions also contribute to the scattering. Our approach leads to the determination of the pure spin disorder contribution to the resistivity. The departure to the model observed for Ni above $T_c/2$ hints that Stoner excitations and the existence of an optical magnon branch become important in the high-temperature regime. Our approach can be extended to other magnets like weak ferromagnets or half-metallic ferromagnets to probe the spin disorder and their coupling to the conductivity.

APPENDIX

In this appendix, we evaluate $L_{ss}(T,B)$, $M_{ss}(T,B)$, $L_{dd}(T,B)$, $M_{dd}(T,B)$, and $M_{sd}(T,B)$ starting from results obtained in Ref. 15. The integrals over the accessible q spin waves give rise to new expressions which express the magnon mass renormalization, the field-induced gap in the magnon spectrum, and the *d*-band splitting:

$$L_{\alpha\alpha}(T,B)=\left(\frac{kTV^2\pi S}{N\hbar k_\alpha^4 a^4}\right)\Phi_\alpha^2 n_\alpha^2 G_{\alpha\alpha}^2 2\mathcal{T}_{\alpha\alpha}(T,B), \quad \text{(A1)}$$

$$M_{ss}(T,B)=\left(\frac{kTV^2\pi S}{N\hbar k_s^3 k_d a^4}\right)\Phi_s^2 n_s n_d G_{sd}^2 4k_s^2 a^2 \mathcal{R}_{sd}(T,B), \quad \text{(A2)}$$

$$M_{dd}(T,B)=\left(\frac{kTV^2\pi S}{N\hbar k_d^3 k_s a^4}\right)\Phi_d^2 n_s n_d G_{sd}^2 4k_d^2 a^2 \mathcal{R}_{sd}(T,B), \quad \text{(A3)}$$

$$M_{sd}(T,B)=\left(\frac{kTV^2\pi S}{N\hbar k_s^2 k_d^2 a^4}\right)\Phi_s\Phi_d n_s n_d G_{sd}^2 \times[-2\mathcal{T}_{sd}(T,B)+2(k_s^2a^2+k_d^2a^2)\mathcal{R}_{sd}(T,B)]. \quad \text{(A4)}$$

The functions $\mathcal{T}_\alpha(T,B)$, $\mathcal{T}_{sd}(T,B)$, and $\mathcal{R}_{sd}(T,B)$ are integrals over the accessible q vectors defined by

$$\mathcal{T}_{\substack{dd\\sd}}^{ss}(T,B)=\frac{a^4}{6}\int_{\substack{q_{\min\,dd}\\q_{\min\,sd}}}^{Q} q^3\,\mathrm{csch}\left(\frac{D(T)q^2+g\mu_B B}{2kT}\right)dq, \quad \text{(A5)}$$

$$\mathcal{R}_{sd}(T,B)=\frac{a^4}{6}\int_{a_{\min\,sd}}^{Q} q\,\mathrm{csch}\left(\frac{D(T)q^2+g\mu_B B}{2kT}\right)dq. \quad \text{(A6)}$$

The Q vector is the maximum accessible magnon wavelength equal to $2k_F$. The low limits for the q integrations are

0, $q_{\min dd}$, and $q_{\min sd}$ for the intraband $s^{\mp}$-$s^{\pm}$ and $d^{\mp}$-$d^{\pm}$ and interband $s^{\mp}$-$d^{\pm}$ electronic transitions, respectively. We neglect the exchange splitting for the s^{+} and s^{-} bands. The $q_{\min dd}$ and $q_{\min sd}$ wave vectors represent the minimum gaps in k space between the d^{+}-d^{-} and s-d bands. Assuming a $2G_{dd}S$ energy exchange splitting for the d-polarized bands, the minimum q vectors are[15,18]

$$q_{\min dd}a = |k_{F_{d^+}} - k_{F_{d^-}}|a \approx \frac{G_{dd}Sk_{Fd}a}{E_F}, \tag{A7}$$

$$q_{\min sd}a = |k_{F_s} - k_{F_d}|a \approx \sqrt{\frac{m_d}{m_s}}\frac{G_{sd}S(k_{F_s}+k_{F_d})a}{2E_F}. \tag{A8}$$

*Corresponding author. FAX: (33) 5 62 28 17 16. Electronic address: raquet@insa-tlse.fr

[1] J. C. Slater, Phys. Rev. **49**, 537 (1936); **49**, 931 (1936).
[2] N. F. Mott, Proc. Phys. Soc. London **47**, 571 (1935).
[3] E. C. Stoner, Proc. R. Soc. London, Ser. A 372 (1938); J. Phys. Radium **12**, 372 (1951).
[4] C. Herring and C. Kittel, Phys. Rev. **81**, 869 (1951).
[5] D. M. Edwards, Phys. Lett. **27A**, 183 (1970).
[6] M. Shimizu, Physica B **91**, 14 (1977).
[7] J. Mathon and E. P. Wohlfarth, Proc. R. Soc. London, Ser. A **302**, 409 (1968).
[8] M. W. Stringfellow, J. Phys. C **2**, 950 (1968).
[9] H. A. Mook and D. McK. Paul, Phys. Rev. Lett. **54**, 227 (1958).
[10] D. McK. Paul, P. W. Mitchell, H. A. Mook, and U. Steigenberger, Phys. Rev. B **38**, 580 (1988).
[11] K. N. Trohidou, J. A. Blackman, and J. F. Cooke, Phys. Rev. Lett. **67**, 2561 (1991).
[12] J. M. Teresa, A. Barthélémy, A. Fert, J. P. Contour, R. Lyonnet, F. Montaigne, P. Seneor, and A. Vaurès, Phys. Rev. Lett. **82**, 4288 (1999).
[13] M. Viret, Y. Samson, P. Warin, A. Marty, F. Ott, E. Sondergard, O. Klein, and C. Fermon, Phys. Rev. Lett. **85**, 3962 (2000).
[14] T. Kasuya, Prog. Theor. Phys. **16**, 58 (1956).
[15] D. A. Goodings, Phys. Rev. **132**, 542 (1963).
[16] D. L. Mills and P. Lederer, J. Phys. Chem. Solids **27**, 1805 (1966).
[17] G. Taylor, A. Isin, and R. V. Coleman, Phys. Rev. **165**, 621 (1968).
[18] A. Fert, J. Phys. C **2**, 1784 (1969).
[19] D. L. Mills, A. Fert, and I. A. Campbell, Phys. Rev. B **4**, 196 (1971).
[20] B. Loegel and F. Gautier, J. Phys. Chem. Solids **32**, 2723 (1971).
[21] H. Yamada and S. Takada, J. Phys. Soc. Jpn. **34**, 51 (1973).
[22] N. V. Volkenshtein, V. P. Dyakina, and V. E. Startsev, Phys. Status Solidi B **57**, 9 (1973).
[23] A. Fert and I. A. Campbell, J. Phys. F: Met. Phys. **6**, 849 (1976).
[24] N. F. Mott, Adv. Phys. **13**, 325 (1964).
[25] W. G. Baber, Proc. R. Soc. London, Ser. A **158**, 383 (1936).
[26] A. B. Pipard, *Magnetoresistance in Metals* (Cambridge University Press, Cambridge, England, 1989).
[27] P. Kapitza, Proc. R. Soc. London, Ser. A **123**, 292 (1929).
[28] H. H. Potter, Proc. R. Soc. London, Ser. A **1931**, 560.
[29] S. N. Kaul and M. Rosenberg, Phys. Rev. B **27**, 5698 (1983).
[30] K. B. Vlasov and V. V. Ustino, Low Temp. Phys. **22**, 728 (1996) and references therein.
[31] E. P. Wohlfarth, Phys. Lett. **3**, 17 (1962).
[32] R. Gersdorf, J. Phys. Radium **23**, 726 (1962).
[33] R. Pauthenet, in *High Field Magnetism*, edited by M. Date (North-Holland, Amsterdam, 1983), p. 77.
[34] S. Hatta, M. Matsui, and S. Chikagumi, Physica B **86–88**, 309 (1977).
[35] D. Fekete, A. Grayevskey, D. Shaltiel, U. Goebel, E. Dormann, and N. Kaplan, Phys. Rev. Lett. **36**, 1566 (1976).
[36] S. V. Halilov, H. Eschrig, A. Y. Perlov, and P. M. Oppeneer, Phys. Rev. B **58**, 293 (1998).
[37] L. Colquitt, Phys. Rev. **139**, A1857 (1965).
[38] C. E. Moore, *Atomic Energy Levels*, National Bureau of Standards Circular No. 467 (U.S. GPO, Washington, D.C., 1952), Vol. 2.
[39] K. Yosida, Phys. Rev. **106**, 893 (1957).
[40] K. Yosida, Phys. Rev. **106**, 893 (1957).
[41] C. Haas, Phys. Rev. **168**, 531 (1968).
[42] R. B. Muniz, J. F. Cook, and D. M. Edwards, J. Phys. F: Met. Phys. **15**, 2357 (1985).
[43] M. van Schilfgaarde and V. P. Antropov, J. Appl. Phys. **85**, 4827 (1999).
[44] T. G. Phillips, Proc. R. Soc. London, Ser. A **292**, 224 (1966).
[45] J. M. Karanikas, R. Sooryakumar, G. A. Prinz, and B. T. Jonker, J. Appl. Phys. **69**, 6120 (1991).
[46] X. Liu, M. M. Steiner, R. Sooryakumar, G. A. Prinz, R. F. C. Farrow, and G. Harp, Phys. Rev. B **53**, 12 166 (1996).
[47] G. Shirane, V. J. Minkiewicz, and R. Nathans, J. Appl. Phys. **39**, 383 (1968).
[48] T. G. Perring, A. D. Taylor, and G. L. Squires, Physica B **213&214**, 348 (1995).
[49] D. M. Edwards and R. B. Muniz, J. Phys. F: Met. Phys. **15**, 2339 (1985) and references therein.
[50] T. Izumaya and R. Kubo, J. Appl. Phys. **35**, 1074 (1964).